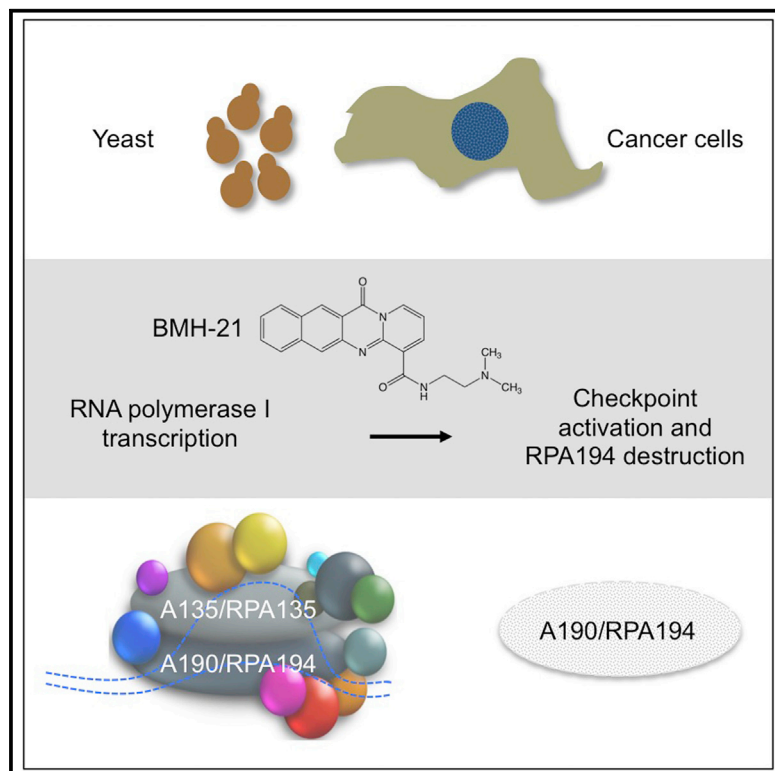# Small-Molecule Targeting of RNA Polymerase I Activates a Conserved Transcription Elongation Checkpoint

Graphical Abstract

Authors

Ting Wei, Saman M. Najmi, Hester Liu, Karita Peltonen, Alena Kucerova, David A. Schneider, Marikki Laiho

Correspondence

mlaiho1@jhmi.edu

In Brief

Targeting of RNA polymerase I is currently being explored for cancer therapeutics. Wei et al. show that small-molecule BMH-21 activates a conserved RNA polymerase I checkpoint that monitors efficiency of transcription. Transcription inhibition and checkpoint activation by BMH-21 disengages the polymerase from chromatin and causes enzyme destruction.

Highlights

- BMH-21 is an RNA polymerase I elongation inhibitor

- Its activity as a polymerase inhibitor is conserved in yeast

- Degradation of the largest subunit reveals a transcription checkpoint

- Elongation defects sensitize cells to polymerase inhibition

Small-Molecule Targeting of RNA Polymerase I Activates a Conserved Transcription Elongation Checkpoint

Ting Wei,[1] Saman M. Najmi,[2] Hester Liu,[3] Karita Peltonen,[1] Alena Kucerova,[1] David A. Schneider,[2] and Marikki Laiho[1,3,4,*]

[1]Division of Pharmaceutical Biosciences, Faculty of Pharmacy and Institute of Biotechnology, University of Helsinki, Helsinki 00014, Finland
[2]Department of Biochemistry and Molecular Genetics, University of Alabama at Birmingham, Birmingham, AL 35294, USA
[3]Department of Radiation Oncology and Molecular Radiation Sciences and Sidney Kimmel Comprehensive Cancer Center, Johns Hopkins University School of Medicine, Baltimore, MD 21231, USA
[4]Lead Contact
*Correspondence: mlaiho1@jhmi.edu
https://doi.org/10.1016/j.celrep.2018.03.066

SUMMARY

Inhibition of RNA polymerase I (Pol I) is a promising strategy for modern cancer therapy. BMH-21 is a first-in-class small molecule that inhibits Pol I transcription and induces degradation of the enzyme, but how this exceptional response is enforced is not known. Here, we define key elements requisite for the response. We show that Pol I preinitiation factors and polymerase subunits (e.g., RPA135) are required for BMH-21-mediated degradation of RPA194. We further find that Pol I inhibition and induced degradation by BMH-21 are conserved in yeast. Genetic analyses demonstrate that mutations that induce transcription elongation defects in Pol I result in hypersensitivity to BMH-21. Using a fully reconstituted Pol I transcription assay, we show that BMH-21 directly impairs transcription elongation by Pol I, resulting in long-lived polymerase pausing. These studies define a conserved regulatory checkpoint that monitors Pol I transcription and is activated by therapeutic intervention.

INTRODUCTION

RNA polymerase I (Pol I) is a highly active enzyme compartmentalized in the nucleolus, where it synthesizes the most abundant RNA species in the cell, the rRNAs (McStay and Grummt, 2008). Transcription of rDNA by Pol I is the first, rate-limiting step in ribosome biogenesis (Haag and Pikaard 2007; Russell and Zomerdijk 2006). The rate of ribosome biosynthesis is proportional to cell growth and proliferation (Grummt 2010; Warner et al., 2001). The relationship between ribosome synthesis and aggressive cancer cell growth has been appreciated for more than a century and was initially described by observation of enlarged nucleoli in tumor cells (Montanaro et al., 2008). More recently, factors driving Pol I transcription in cancers have been identified. These include oncogenic activity by Myc, Ras/ERK, mTOR, and Akt/PKB and loss of Pol I repression by tumor suppressors p53, Rb, ARF, and PTEN genomic alterations (Bywater et al., 2013;

Drygin et al., 2010). Despite the abundance of data showing deregulation of Pol I transcription in human cancers, Pol I has been an underexplored target for selective inhibition of cancer cell growth. Recent identification of several small-molecule inhibitors of Pol I (BMH-21, BMH-9, BMH-22, BMH-23, CX-5461, and ellipticine) have provided new tools to assess the links between Pol I transcription and cancer growth (Andrews et al., 2013; Bywater et al., 2012; Drygin et al., 2011; Morgado-Palacin et al., 2014; Peltonen et al., 2014a, 2014b). Studies in vitro and in mouse models have shown therapeutic efficacy by the rRNA transcription inhibitors (Bywater et al., 2012; Drygin et al., 2011; Peltonen et al., 2014a). Translation of these advances to cancer care will require identification of the mechanisms by which the inhibitors influence Pol I.

We discovered the small-molecule BMH-21 in a high-throughput screen for anticancer agents (Peltonen et al., 2010). BMH-21 blocks Pol I transcription rapidly and profoundly and induces proteasome-mediated degradation of the largest subunit of Pol I, RPA194 (Peltonen et al., 2014a). This effect is unique to BMH-21 and is not observed by other inhibitors that affect Pol I (CX-5461, actinomycin D, topoisomerase I, and II poisons) (Peltonen et al., 2014a). BMH-21 binds GC-rich DNA in a non-covalent, charge-dependent manner without activating a DNA damage response (Colis et al., 2014a; Peltonen et al., 2010, 2014a). We have shown that BMH-21 causes destabilization of RPA194 in a manner independent of several DNA damage and replication checkpoint kinases (Colis et al., 2014a; Peltonen et al., 2014a). Furthermore, the degradation of RPA194 correlates with BMH-21-mediated cancer cell death. These findings indicate that degradation of RPA194 may reflect a regulatory step in Pol I transcription and be of therapeutic value.

The large subunit of Pol II, Rpb1, is degraded in response to stalled transcription complexes, and this pathway is considered a regulatory process by which cells resolve transcription elongation blocks (Wilson et al., 2013). BMH-21 does not affect Rpb1 under conditions in which RPA194 is degraded, but on the other hand, cell stresses that cause Rpb1 degradation do not affect RPA194 (Peltonen et al., 2014a). Thus, the pathways that monitor transcription and induce degradation of Pols I and II are distinct.

Pols I and II are structurally and functionally related multisubunit polymerases (Engel et al., 2013; Fernández-Tornero et al., 2013; Martinez-Rucobo and Cramer 2013). We recently
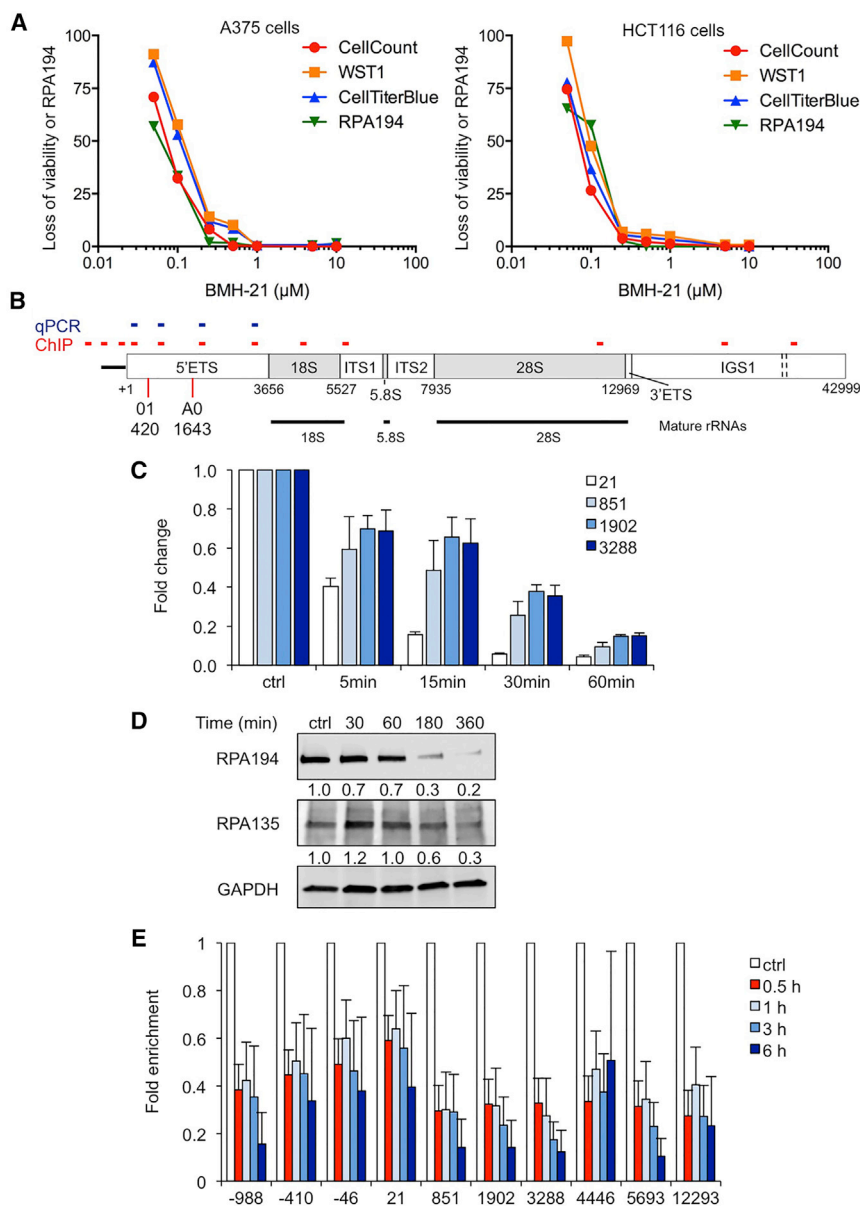
Figure 1. Rapid Inhibition of Pol I Transcription and Dissociation of Pol I from rDNA

(A) A375 and HCT116 cells treated with increasing doses of BMH-21 for 72 hr were analyzed by cell counting, WST1, and CellTiter Blue viability assays. Expression of nucleolar RPA194 was analyzed using immunofluorescence and quantitative analysis.

(B) Diagram of human rRNA coding locus and location of qPCR and ChIP primers.

(C) A375 cells were treated with BMH-21 (1 μM) for the indicated times, and rRNA synthesis was analyzed by qRT-PCR using primers for short-lived 5′ETS (5′-external transcribed spacer) rRNA. 5′ETS primer locations as shown in (B). Mean ± SEM of n = 5 biological replicates are shown.

(D) A375 cells were treated with BMH-21 (1 μM) for the indicated times followed by western blotting analysis for RPA194 and RPA135.

(E) RPA194 ChIP-qPCR of A375 cells treated with BMH-21 (1 μM) for the indicated times. Primer locations are shown in (B). Data are represented as mean ± SEM of n = 3 biological replicates.

See also Figure S1.

impaired are hypersensitive to BMH-21, supporting the idea that BMH-21, at least in part, directly affects Pol I transcription. Finally, we use fully reconstituted transcription assays *in vitro* to demonstrate that BMH-21 directly inhibits Pol I transcription elongation, inducing pausing. These findings reveal a new, conserved Pol I-specific transcription checkpoint.

RESULTS

Rapid Inhibition of Pol I and Clearance of the Enzyme from rDNA

We have shown that inhibition of Pol I by BMH-21 activates a unique cellular response resulting in the degradation of RPA194 and that this degradation correlates with its effectiveness to decrease cancer cell viability (Peltonen et al., 2014a). To define the cellular response to BMH-21 in more detail, we treated two cancer cell lines with increasing concentrations of BMH-21 and tested for loss of cell viability using three different readouts for cellular activity (mitochondrial membrane potential, protein content, and cell number) and compared those data with the nucleolar abundance of RPA194. We found that loss of RPA194 tightly correlated with decreased cell fitness in all assays after treatment with BMH-21 (Figure 1A).

To describe the kinetics of the response to BMH-21, we treated A375 cells with 1 μM BMH-21 and measured rRNA synthesis and Pol I occupancy of the rDNA. The 5′-external transcribed spacer (5′ETS) precursor is cleaved from the primary rRNA transcript by early and rapid processing steps (01 and A1) (Figure 1B), resulting in a short-lived RNA species whose

published that Pols I and II have evolved divergent enzymatic properties, resulting in potentially different rate-limiting steps during transcription elongation (Schneider 2012; Viktorovskaya et al., 2013). These findings led us to test the hypothesis that BMH-21 impairs transcription elongation by Pol I. We find that BMH-21 leads to rapid clearance of Pol I from rDNA and that this effect depends on efficient transcription initiation. We show that RPA194 is stabilized by association with RPA135, the second largest catalytic subunit, and depletion of RPA135 prevents degradation of RPA194 in the presence of BMH-21. Remarkably, the effects of BMH-21 on Pol I are conserved in *Saccharomyces cerevisiae* (brewer's yeast). BMH-21 treatment results in decreased Pol I transcription, degradation of A190 (the RPA194 homolog), and reduced cell viability. Furthermore, yeast strains in which Pol I transcription elongation is selectively

abundance is generally reflective of the rRNA synthesis rate (Mullineux and Lafontaine 2012; Popov et al., 2013). We measured 5′ETS precursor abundance using several primer pairs by qPCR in cells treated with BMH-21 for 5, 15, 30, and 60 min (Figures 1B and 1C). We observed rapid (within 5 min) decrease of the 5′ETS transcripts that was especially prominent using primers for the short-lived 5′ end of the ETS transcript (upstream of the 01 cleavage site). The decrease of the 5′ETS transcripts downstream of the 01 cleavage site was slower, consistent with their longer half-lives (Figure 1C). Regardless of the 5′ETS primer used, a prominent inhibition of transcription was observed within 1 hr.

We then assessed Pol I occupancy of the rDNA after BMH-21 treatment using chromatin immunoprecipitation (ChIP). Given that we have previously shown that BMH-21 decreases the half-life of RPA194 from more than 20 hr to approximately 1 hr (Peltonen et al., 2014a), we first determined the abundance of RPA194 by western blotting over a time course relevant for this study. BMH-21 caused a prominent decrease of RPA194 within 3 hr (Figure 1D). In addition, we observe some decrease in RPA135, in accordance with our previous findings (Peltonen et al., 2014a). We then performed ChIP qPCR of cells treated with BMH-21 for 0.5, 1, 3, or 6 hr using primers throughout the gene body. The data showed that RPA194 was disengaged from both the promoter and coding regions of the rDNA within 30 min of treatment (Figure 1E). Thus, the kinetics of loss of RPA194 chromatin engagement was faster than the protein's degradation.

We have shown that the turnover of RPA194 is dependent on the proteasome (Peltonen et al., 2014a). To further assess whether the loss of Pol I chromatin engagement results from its turnover, we treated cells with BMH-21 and MG132, a proteasome inhibitor. As assessed by immunofluorescence and western blotting, and consistent with our previous observations, MG132 abolished the decrease in RPA194 by BMH-21 and led to substantial accumulation of RPA194 and the second largest subunit, RPA135, in the nucleolar caps (Figures S1A and S1B).

We then conducted ChIP-qPCR of cells treated with BMH-21 and MG132. Treatment of cells with MG132 somewhat increased RPA194 on the gene body (Figure S1C). Enrichment of RPA194 on the gene body following co-treatment of cells with BMH-21 and MG132 was similar to the control (Figure S1C). This finding suggests that BMH-21 causes loss of RPA194 from rDNA in a manner that is at least partially dependent of RPA194 turnover.

Depletion of the Preinitiation Complex Factors Rescues RPA194 Degradation

We hypothesized that BMH-21 impairs transcribing Pol I complexes. If engaged Pol I transcription complexes are targets of BMH-21-mediated protein turnover, then efficient transcription initiation would be required to observe degradation of RPA194. To test this hypothesis, we silenced factors required for transcription initiation by Pol I: UBF, RRN3, and TAF$_I$110. For each depletion, two independent small interfering RNAs (siRNAs) were used against each gene, and the depletion was confirmed by western blotting (Figure 2) and qPCR (not shown). We then

treated the cells with BMH-21 and assessed changes in abundance of RPA194 by western blotting and immunofluorescence. As shown in Figure 2, depletion of each transcription initiation factor led to rescue of RPA194 abundance in the BMH-21-treated cells. Yet BMH-21 decreased Pol I transcription in the knockdown cells, as shown by 5′ETS qPCR and markers of nucleolar stress in UBF-depleted cells, showing that transcription inhibition alone was insufficient to cause RPA194 loss (Figure S2). The findings suggested that degradation of RPA194 requires efficient loading of Pol I onto the rDNA.

BMH-21 Causes Cytoplasmic Redistribution of RPA135

The two largest Pol I subunits, RPA135 and RPA194, associate and form the active center of Pol I (Engel et al., 2013; Fernández-Tornero et al., 2013; Schneider and Nomura, 2004). We have shown that although RPA194 is dramatically depleted after treatment with BMH-21, RPA135 abundance is only mildly affected (Peltonen et al., 2014a). To identify the fate of RPA135 after treatment, we analyzed the effect of BMH-21 on RPA135 cellular distribution. Using immunofluorescence followed by quantitative analysis, we observed that RPA135 nucleolar localization was decreased over time (Figures 3A and 3B). The kinetics of loss of RPA135 from the nucleolus was similar to that of RPA194 (Figures 3C and 3D) (Peltonen et al., 2014a). Fractionation of cellular extracts showed that BMH-21 caused obvious relocation of RPA135 into the cytoplasm, whereas RPA194 abundance decreased in both cytoplasm and nucleoplasm (Figures 3E and 3F). These changes were evident already within 30 min of exposure to BMH-21 and coincided with the observed decrease in Pol I occupancy of the rDNA after treatment (Figure 1E).

We show in Figure 2A that RPA194 and RPA135 were retained in the nucleolar caps following treatment with BMH-21 and MG132. To assess the distribution of the Pol I proteins biochemically, we conducted cellular fractionation of cells treated in the presence or absence of BMH-21 and MG132 for 3 hr. The cytoplasmic translocation of RPA135 was again evident following exposure to BMH-21, but this effect was abrogated by MG132 (Figure 3G). Together, these data show that BMH-21 treatment results in degradation of RPA194, but redistribution of RPA135, suggesting that RPA135 nucleolar localization depends on RPA194.

RPA135 Is Requisite for the Stability of RPA194

On the basis of the above findings, it is reasonable to expect that dissociation of RPA194 from RPA135 may reduce RPA194 stability while at the same time affecting RPA135 distribution. To test this model, we examined the effects of RPA135 depletion on RPA194 abundance. RPA135 transcript and protein were effectively decreased by siRNA treatment (Figures 4A–4D). Strikingly, the depletion of RPA135 also led to a pronounced decrease in RPA194, as shown by immunofluorescence analysis and western blotting (Figures 4B–4D). Furthermore, we did not observe any further decrease in RPA194 by BMH-21 in the RPA135-depleted cells (Figures 4C and 4D), consistent with the model that only transcriptionally active Pol I complexes are subject to BMH-21-induced degradation. These data show that RPA194 is unstable in the absence of RPA135.
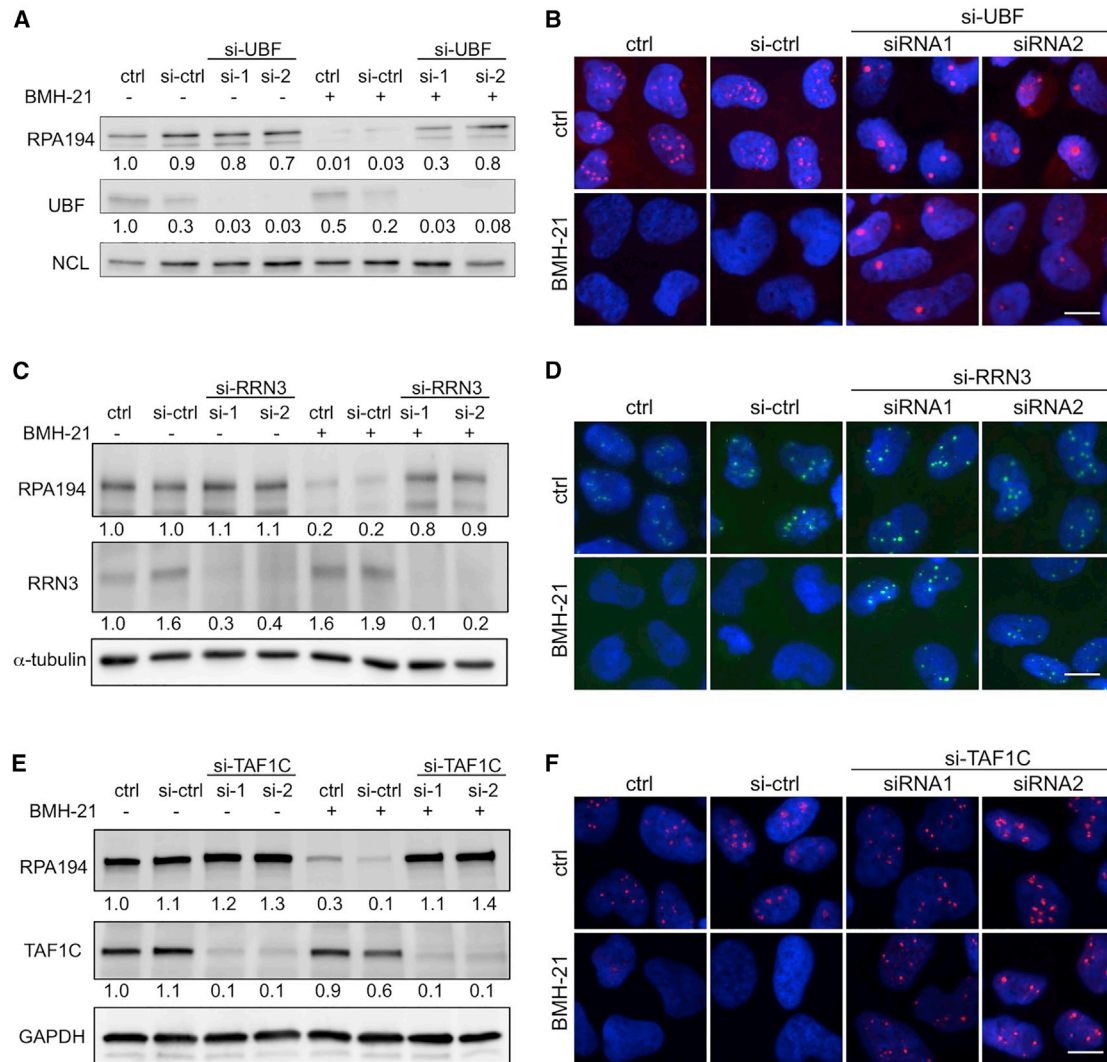
Figure 2. Depletion of the Preinitiation Factors Rescues RPA194 Degradation by BMH-21

(A and B) A375 cells were transfected with two siRNAs targeting UBF, incubated for 72 hr, and treated with BMH-21 for 3 hr. (A) Western blotting for UBF, RPA194, and NCL as loading control. Representative blots of n = 2 experiments. (B) Immunofluorescence analysis for RPA194. Merged images (RPA194, red; DNA, blue) are shown. Scale bar, 10 μm.

(C and D) Depletion of RRN3 using siRNAs. A375 cells were transfected with two siRNAs targeting RRN3, incubated for 72 hr, and treated with BMH-21 for 3 hr. (C) Western blotting for RRN3, RPA194, and α-tubulin as loading control. Representative blots of n = 2 experiments. (D) Immunofluorescence analysis for RPA194. Merged images (RPA194, green; DNA, blue) are shown. Scale bar, 10 μm.

(E and F) Depletion of TAF1C using siRNAs. A375 cells were transfected with two siRNAs targeting TAF1C, incubated for 72 hr, and treated with BMH-21 for 3 hr. (E) Western blotting for TAF1C, RPA194, and GAPDH as loading control. Representative blots of n = 4 experiments. (F) Immunofluorescence analysis for RPA194. Merged images (RPA194, red; DNA, blue) are shown. Scale bar, 10 μm.

See also Figure S2.

Degradation of the Largest Pol I Subunit Is Conserved among Eukaryotes

To test whether the effect of BMH-21 on rRNA synthesis is conserved among eukaryotes, we exposed exponentially growing *Saccharomyces cerevisiae* cells to 50 μM BMH-21 and measured rRNA synthesis and A190 abundance (the yeast homolog of RPA194). To measure rRNA synthesis, we measured the abundance of pre-rRNA segments ITS1 or 5′ETS. These pre-rRNA segments are rapidly processed after their synthesis, so intact pre-RNA measured is indicative of newly synthesized rRNA. We found that BMH-21 caused a robust, rapid inhibition of rRNA synthesis (Figure 5A) and degradation of A190 (Figure 5B). These data suggest that the cellular response to BMH-21 is conserved across eukaryotic species.

Because the effects of BMH-21 are conserved, we took advantage of the genetic capabilities of the yeast system to test the model that BMH-21 targets the Pol I transcription elongation complex. Previous studies have identified point mutations
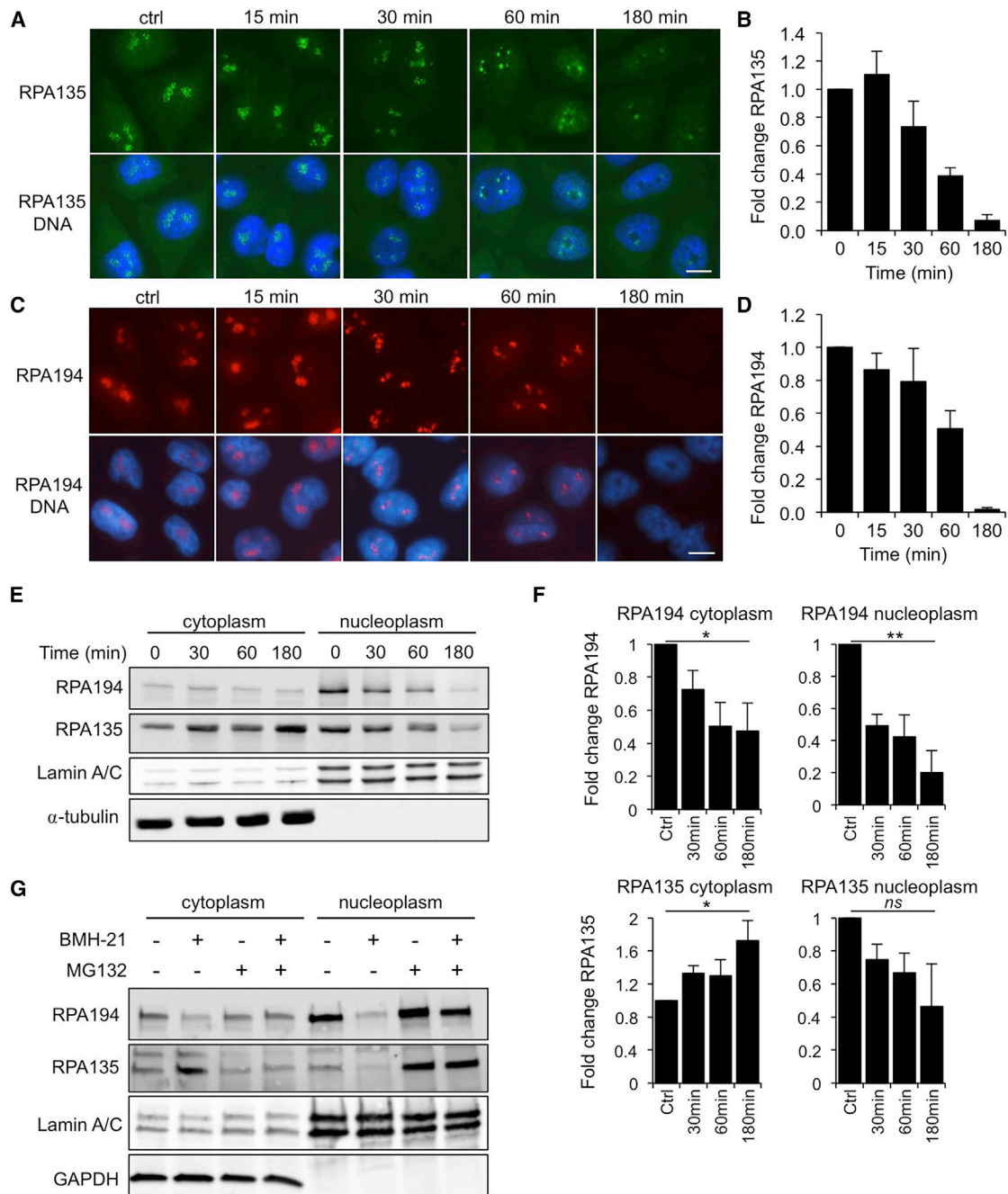
Figure 3. BMH-21 Causes RPA135 Cellular Redistribution

(A and C) A375 cells were incubated with BMH-21 (1 μM) for the given times, followed by staining of the fixed cells for RPA135 (A, green) or RPA194 (C, red) and counterstaining for DNA (blue). Scale bar, 10 μm.

(B and D) Quantitative image analysis of nucleolar RPA135 (B, n = 4 biological replicates) or RPA194 (D, n = 5 biological replicates). Mean and SEM are shown.

(E) Western blotting analysis of RPA194 and RPA135 in cytoplasmic and nucleoplasmic fractions. Loading controls are lamin A/C and α-tubulin.

(F) Quantification of n = 3 biological experiments in (E). Data are represented as mean ± SD; p value, Dunnett's multiple comparison test. ns, non-significant; *p < 0.05; **p < 0.01.

(G) A375 cells were incubated with BMH-21 (1 μM) and/or MG132 (10 μM) for 3 hr followed by cellular fractionation and western blotting analysis for RPA194 and RPA135. Loading controls are lamin A/C and GAPDH.
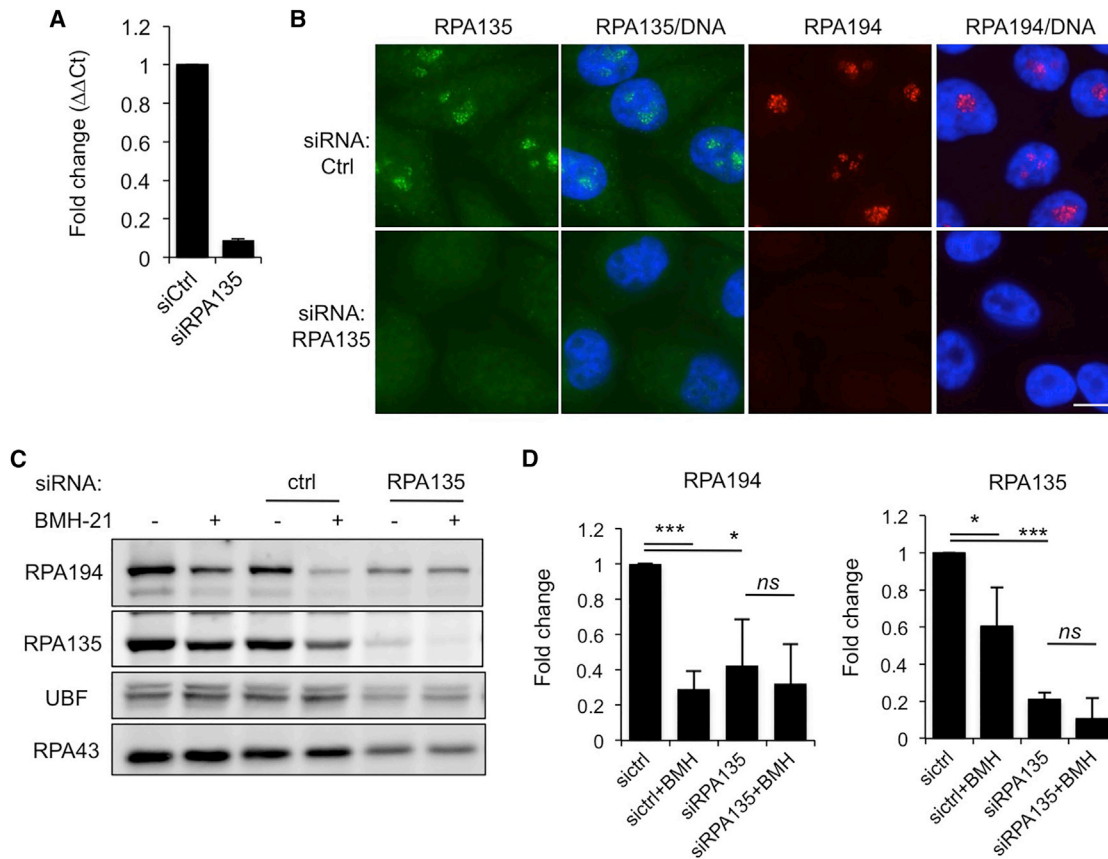
Figure 4. RPA135 Is Requisite for the Stability of RPA194

(A) A375 cells were transfected with control siRNAs or siRNAs targeting RPA135 and incubated for 48 hr, and RPA135 transcript was analyzed by qPCR. Fold change is shown.

(B) Immunofluorescence staining of cells treated as in (A) for RPA135 (green) and RPA194 (red) and counterstained for DNA (blue). Scale bar, 10 μm.

(C) RPA135 was depleted using siRNAs. Cells were incubated for 72 hr following transfection with the siRNAs and then treated with BMH-21 (1 μM) for 3 hr. Western blotting for RPA135, RPA194, and UBF and A43 as a loading controls.

(D) Quantification of n = 3 biological experiments in (C). Data are represented as mean ± SD; p, Student's two-tailed t test. ns, non-significant; *p < 0.05; ***p < 0.001.

that impair individual steps in transcription by Pol I. Here, we used two mutations that were identified for their negative effects on transcription elongation by Pol I (*rpa135-D784G* and *rpa190-F1205H*; Schneider et al., 2007; Viktorovskaya et al., 2013). We also used a mutation in the *RRN3* gene that selectively impairs transcription initiation (*rrn3-S213P*; Claypool et al., 2004). We exposed these mutant cells, as well as wild-type (WT) controls, to BMH-21 and measured cell viability, rRNA synthesis, and A190 abundance. We found that both "elongation" mutants were hypersensitive to BMH-21, consistent with a role for the compound during the elongation phase of transcription (Figure 6A). These mutants also displayed clear inhibition of rRNA synthesis and degradation of A190, similarly to WT (Figures 6B and 6C). On the other hand, when transcription initiation by Pol I is impaired because of the *rrn3* mutant allele, we found that the cells' viability in response to BMH-21 was comparable with the WT, rRNA synthesis was inhibited, but A190 was not robustly degraded. These observations are consistent with data collected using mammalian cells (Figure 2) and with the model

that Pol I transcription elongation complexes are the substrate for Pol I subunit degradation after exposure to BMH-21.

BMH-21 Directly Inhibits Transcription Elongation by Pol I

These genetic and molecular data suggest that BMH-21 inhibits transcription elongation by Pol I. To test this model directly, we used a fully reconstituted transcription elongation assay for Pol I in the presence and absence of BMH-21. We used a modified yeast rDNA template in which C-residues in the initially transcribed region have been mutated to G. Thus, we initiated transcription in the absence of BMH-21 or CTP, synchronized elongation complexes downstream of the promoter at the first encoded C (position +56), and we split the reaction. To half of the reaction, we added 1 μM BMH-21, and to the other, we added a vehicle control (DMSO). Finally, we added heparin to both reactions to serve as a trap and ensure single turnover reaction conditions. After the addition of CTP, we collected samples as a function of time. RNA products were resolved on
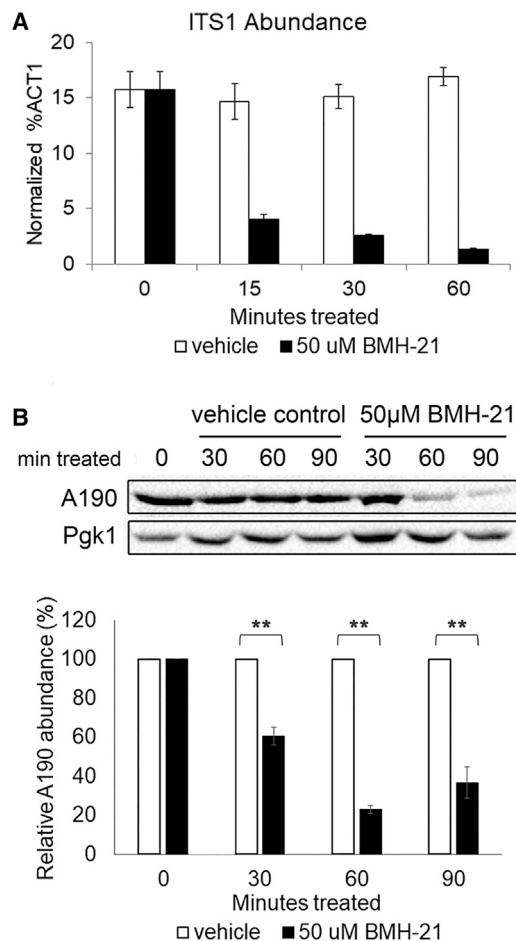
A ITS1 Abundance

B

Figure 5. BMH-21 Effect on Pol I Is Conserved in Yeast

(A) Cells were grown in YEPD and treated with 50 μM BMH-21 for indicated times and harvested. RNA was purified and analyzed with RT-qPCR using primers targeting the pre-rRNA segment ITS1, the abundance of which is indicative of newly synthesized rRNA, and to ACT1 mRNA, for normalization purposes. Data shown are representative of n = 3, and error bars represent SD of technical replicates.

(B) Cells were grown in YEPD and treated with 50 μM BMH-21 for indicated times. Cells were harvested, lysed, and analyzed for A190 and Pgk1 abundance with western blot analysis. Data shown are averages of n = 3, and error bars represent SEM of biological replicates. Significance was calculated using one-way ANOVA. **p < 0.01.

polyacrylamide gels and visualized by phosphorimaging. A representative gel is displayed in Figure 7A and quantification in Figure 7B. The addition of BMH-21 to the elongation complexes induced the accumulation of shorter products that represent major pause sites in the template. Consistent with the appearance of these paused populations, we observed much slower accumulation of the full-length product. Thus, BMH-21 directly inhibits transcription elongation by Pol I. In addition to the dramatic effect of BMH-21 on transcription elongation rate, we observed a modest (~20%) decrease in the amount of full-length product accumulation. This observation suggests that BMH-21 directly induces either premature termination or irreversible arrests of transcription elongation complexes. Together,

all of these biochemical observations are consistent with the data collected from cell lines and in yeast strains supporting a role for BMH-21 in direct inhibition of Pol I transcription complexes.

DISCUSSION

Our studies show that BMH-21 inhibits rRNA synthesis in cancer cells rapidly and robustly. The inhibition of rRNA synthesis leads to proteasome-dependent degradation of the largest subunit of Pol I, RPA194 (Peltonen et al., 2014a). The rapid degradation of RPA194 closely correlated with decreased cancer cell survival in response to BMH-21. In order to understand the basis of this previously unknown degradation pathway for Pol I, it was necessary to identify how BMH-21 targets Pol I transcription. We show here that BMH-21 causes rapid inhibition of Pol I transcription and decreased occupancy of Pol I on the rDNA. These rapid kinetic effects are observed before the abundance of RPA194 is robustly decreased. Thus, transcriptionally active Pol I is somehow perturbed or evicted from the rDNA prior to RPA194 degradation. Remarkably, this effect of the compound is conserved in yeast, and mutations that impair transcription elongation by Pol I result in hypersensitivity to BMH-21. Taken together with the fact that Pol I transcription elongation is directly inhibited by BMH-21 *in vitro*, we conclude that BMH-21 can have a direct effect on rRNA synthesis and propose that it activates a conserved pathway that monitors the efficiency of Pol I transcription. Here we use the term "checkpoint" to describe the surveillance of the integrity Pol I transcription. Activation of this "checkpoint" by BMH-21 or potentially other naturally occurring stresses specifically leads to the degradation of the largest subunit of Pol I.

Polymerases frequently encounter lesions or blocks in their templates. In response to unsuccessful resolution of Pol II blocks at DNA lesions, the Pol II subunit Rpb1 is marked for proteasome-mediated degradation (Wilson et al., 2013). The degradation of Rpb1 leads to removal of the Pol II complex from DNA and is considered necessary for cell survival. Our work has identified a similar clearance mechanism for Pol I. We have shown that stimuli that cause destabilization of the large subunits of Pol I and Pol II are different. BMH-21 does not cause degradation of Pol II Rpb1, and conversely, UV that causes Rpb1 destabilization has no effect on RPA194 degradation either in mammalian cells (Peltonen et al., 2014a) or in the yeast (Richardson et al., 2012). The degradation of RPA194 is mediated through the proteasome, and a RPA194 deubiquitinating enzyme has been identified in the mammals (USP36; Peltonen et al., 2014a) and its counterpart Upb10 in yeast (Richardson et al., 2012). In yeast, A190 is particularly prone for degradation at low temperatures when *upb10* is deleted, suggesting activation of the checkpoint also by physiological signals. In order to resolve these transcription blocks, the enzyme is disengaged from rDNA, and RPA194/A190 is marked for degradation. Because the rDNA is one of the most highly transcribed loci in growing cells, BMH-21 is more likely to intercalate into these loci and selectively perturb rDNA transcription. The observed degradation of RPA194 only in the cancer cells, but not in normal cells, further supports this model and identifies the rDNA as a clear vulnerability rapidly proliferating cells.
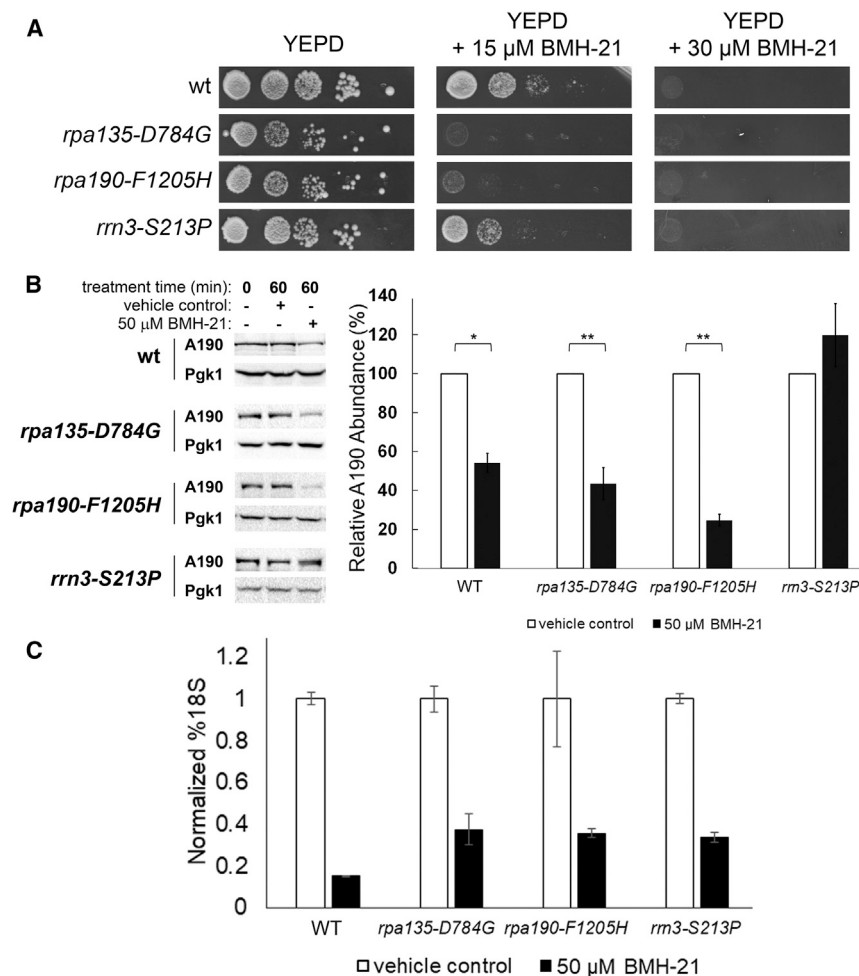
A

B

C

Figure 6. BMH-21 Exposure Results in Defects in Pol I Elongation, and Inhibiting Initiation Rescues A190 Degradation

(A) Cultures were grown in YEPD liquid media and harvested. For the spot assay, 10-fold dilutions were made, the first being 0.1 at A_{600}, and 5 μL were plated on YEPD plates containing indicated concentrations of BMH-21. Plates were incubated at indicated temperatures for 3 days.

(B) Cells were grown in YEPD and treated with 50 μM BMH-21 for 60 min. Cells were harvested, lysed, and analyzed for A190 and Pgk1 abundance with western blot analysis. Data shown are averages of n ≥ 3, and error bars represent SEM of biological replicates. Significance was calculated using one-way ANOVA. *p < 0.05; **p < 0.01.

(C) Cells were grown in YEPD and treated with 50 μM BMH-21 for 30 min and harvested. RNA was purified and analyzed for 5′ETS abundance with RT-qPCR. Data shown are representative of n = 3, and error bars represent SD of technical replicates.

The change in RPA194 half-life by BMH-21 is profound, whereas other Pol I subunits, with the exception of a minor decrease in RPA135, are not affected (Peltonen et al., 2014a). However, the nucleolar abundance of RPA135 decreases and it is relocated in the cytoplasm after treatment with BMH-21. We assessed whether RPA135 affects RPA194 stability. Remarkably, the depletion of RPA135 substantially decreased the abundance of RPA194. Furthermore, BMH-21-mediated degradation of RPA194 was abrogated in cells with RPA135 knockdown. These findings suggest that RPA135 is required for the stability of RPA194 and are concordant with our previous demonstration in yeast that A190 and A135 maintain a stable association through multiple rounds of transcription (Schneider and Nomura 2004). The implication is profound, suggesting that one subunit directly governs the stability of the catalytic core of the enzyme.

The primary pathways regulating ribosome biogenesis are conserved between yeast and mammals. Here, we find a remarkable conservation of the key characteristics of the Pol I inhibitor that includes inhibition of rRNA synthesis, decreased abundance of A190 and loss of yeast fitness. This enabled us to use previously characterized Pol I elongation mutant strains of *A190* and *A135* that have compromised elongation rates yet maintain viability (Schneider et al., 2007; Viktorovskaya et al., 2013). Both mutants, compared with WT and an initiation-impaired *rrn3* mutant strain, displayed increased sensitivity to BMH-21, emphasizing that the Pol I inhibitor particularly hindered the growth of elongation defective cells. Furthermore, BMH-21 decreased the abundance of A190 in the elongation-impaired mutants, but not in the initiation-impaired mutant strain, which was concordant with the regulation of RPA194 turnover observed in the cancer cells. These studies support and promote the concept that the elongation phase of transcription presents a previously unappreciated vulnerability that can be targeted for therapeutic intervention.

There are technical and conceptual limitations of the data and interpretation. For example, Pol I inhibition by BMH-21 may only affect loading of the polymerase at the promoter, or BMH-21 may inhibit promoter escape. Both scenarios would be consistent with the rapid kinetics of inhibition and reduced Pol I rDNA association. However, it would be more difficult to explain how Pol I degradation is induced when these steps are inhibited. We showed that genetic depletion of members of the preinitiation complex does not activate RPA194/A190 degradation, but in contrast, the preinitiation complex is needed for polymerase decay. Hence, polymerase loading is required. These findings do not rule out that BMH-21 blocks promoter escape and need to be addressed in future studies. We note, however, that we do not observe increased Pol I pausing at the promoter on the basis of ChIP. However, ChIP may have technical limitations due to changes in the antigen or accessibility to chromatin, or lack sensitivity because of rapid clearance in detection of paused complexes. Both the *in vitro* and genetic data are consistent with inhibition of elongation activating the depletion of RPA194. However, it also plausible that additional points of intervention exist.
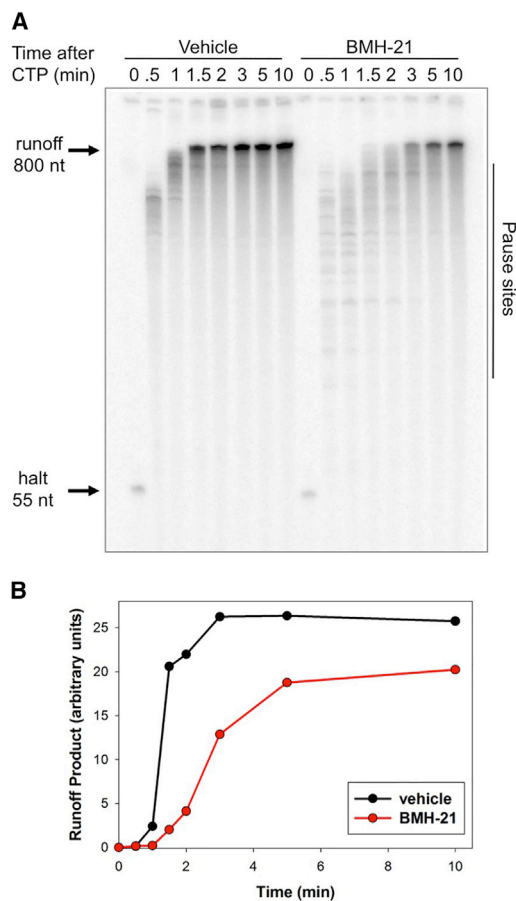
A

Time after
CTP (min)

	Vehicle	BMH-21
	0 .5 1 1.5 2 3 5 10	0 .5 1 1.5 2 3 5 10

runoff
800 nt →

halt
55 nt →

Pause sites

B

Figure 7. BMH-21 Directly Inhibits Pol I Transcription Elongation

(A) Promoter-dependent transcription was performed using purified yeast Pol I and required transcription initiation factors *in vitro*. Transcription was initiated by addition of 200 μM ATP and GTP and 20 μM UTP (+α³²P-UTP), resulting in elongation to the first encoded C residue (at +56). The reaction was split equally, and BMH-21 (1 μM) or an equal volume of DMSO was added to the separate reactions, followed by addition of CTP (200 μM), and samples were collected as a function of time. RNA was purified and run on an 8% acrylamide denaturing gel. The gel was dried, exposed to a phosphor-image screen, and visualized. Positions of relevant RNA products are labeled.

(B) Amount of ³²P-RNA detected in the full-length product was quantified and plotted as a function of time.

The kinetics of the induction of this checkpoint presents another fascinating but complicated question. Transcription of the rDNA is almost fully inhibited within 30 min, and at the same time both RPA194 and RPA135 undergo changes in their localization. The cytoplasmic translocation of RPA135 is prevented by proteasome inhibition, which is indicative that RPA135 localization depends on stability of RPA194. RPA194 half-life is decreased from more than 20 hr to 1 hr (Peltonen et al., 2014a) and is thus lagging behind transcription inhibition. It is possible that this kinetic delay represents a surplus of RPA194/RPA135 complexes and/or that only complexes physically associating with rDNA are targeted for degradation. Inhibition of transcription initiation protects RPA194 from decay but does not rescue rRNA synthesis. Thus, this checkpoint monitors

actively transcribing Pol I complexes. These complexes are somehow marked for degradation and cleared from the DNA. What is the initial mark on the enzyme? Is it ubiquitin? What activates the mark, and are there several marking events as for Pol II? Does the marking require the formation and relocalization of RPA194 to the nucleolar caps observed preceding the degradation? What factors govern this checkpoint? These and other questions must be answered to reveal the mechanism by which eukaryotes monitor and protect the metabolism of the rDNA.

Several chemical tools have recently been described that interfere with Pol I transcription. CX-5461 and ellipticine stabilize G-quadruplex structures and cause DNA damage (Andrews et al., 2013; Brown et al., 2011; Xu et al., 2017). Ellipticine targets the preinitiation complex at the rDNA promoter, and similarly, CX-5461 has been suggested to inhibit the preinitiation complex engagement with the rDNA promoter (Andrews et al., 2013; Drygin et al., 2011). Importantly, several chemotherapeutic agents, such as topoisomerase I and II poisons, inhibit Pol I transcription by blocking rDNA unwinding (Burger et al., 2010). RPA194 abundance or Pol I activity could be potentially useful biomarkers for identification of cancers sensitive to Pol I inhibitor therapies. To facilitate the latter, we have recently developed an RNA probe for the detection of rRNA transcription in paraffin-embedded tumor samples. This probe, detecting the short-lived 5′ETS precursor rRNA, directly reveals the remarkable increase in Pol I activity between benign and carcinoma lesions (Guner et al., 2017). These findings provide impetus for the translation of Pol I inhibitory strategies. Detailed understanding of the mechanisms of action of each drug will be essential for the success of this goal.

EXPERIMENTAL PROCEDURES

Cell Culture and Reagents

A375 melanoma (CRL-1619) and U-2 OS osteosarcoma (HTB-96) cells were from American Type Culture Collection. These cell lines were authenticated using STR analysis by Johns Hopkins Genetic Resources Core Facility and tested periodically for Mycoplasma using qPCR with negative results. The cells were maintained at 37°C in a humidified atmosphere containing 5% CO_2. A375 cells were cultured in DMEM supplemented with 10% fetal bovine serum (FBS) and 4.5 g/L glucose and U-2 OS cells in DMEM with 15% FBS. The reagent used in this study was 12H-benzo[g]pyrido[2,1-b]quinazoline-4-carboxamide, N-[2(dimethylamino)ethyl]-12-oxo (BMH-21), which was synthesized as described by Colis et al. (2014b) and verified for purity using liquid chromatography/mass spectrometry (LC/MS) and ¹H nuclear magnetic resonance (NMR). MG132 was from Sigma-Aldrich and from Enzo LifeSciences.

Viability Assays

Cell viability was determined using WST-1 cell proliferation reagent (Roche Diagnostics), CellTiter Blue cell viability assay (Promega), or by counting the cells using Cellometer Auto T4 (Nexelcom Bioscience LLC).

RNAi

For RNAi using small interfering siRNAs, cells were transfected with 10 nM of targeting gene or negative control siRNAs using Lipofectamine RNAiMAX (Invitrogen), and the cells were incubated for 48–72 hr. The following siRNAs were used: UBTF (115986 and 108497), RRN3 (s29324 and s29325), TAF1C (s17171 and s17172), and POLR1B/RPA135 (s38603 and s38605) (Ambion, Thermo Fisher Scientific).

Immunofluorescence and Image Analysis

For all immunofluorescence procedures, we followed our earlier protocols (Peltonen et al., 2014a). Cells grown on coverslips were fixed in 3.5%

paraformaldehyde or 100% methanol, permeabilized with 0.5% NP-40 lysis buffer (50 mM Tris-HCl [pH 7.5], 150 mM NaCl, 0.5% NP-40, and 50 mM NaF), and blocked in 3% BSA. The following primary antibodies were used: POLR1B/RPA135 (4H6; Santa Cruz Biotechnology), POLR1A/RPA194 (C-1; Santa Cruz Biotechnology), NPM (FC-61991; Invitrogen), NCL (4E2; Abcam), and fibrillarin (ab5821; Abcam). Secondary antibodies used were Alexa 488 and Alexa 594-conjugated anti-mouse and anti-rabbit antibodies (Invitrogen). DNA was stained with Hoechst 33342. Images were captured using DM6000B wide-field fluorescence microscope (Leica). The microscope was equipped with a Hamamatsu Orca-Flash 4.0 V2 sCMOS camera and LAS X software by using 40×/1.25–0.75 HCX PL APO CS oil and 63×/1.40–0.60 HCX PL APO Lbd.bl. oil objectives. Quantitative image analysis of nucleolar protein expression was as described in Peltonen et al. (2014a) and was conducted on at least 200 cells per sample on three to five fields.

Subcellular Fractionation

Cytoplasmic and nucleoplasmic fractions were prepared in the following steps. Cells were lysed with hypotonic buffer (10 mM HEPES [pH 7.9], 1.5 mM $MgCl_2$, 10 mM KCl, 0.5 mM DTT, and protease inhibitors), and 50 μg/mL digitonin was added. Cells were centrifuged at 2,000 × g for 6 min to isolate cytoplasmic fraction, and the cell pellet containing nuclei was subsequently lysed with isotonic buffer (5 mM HEPES [pH 8.0], 1.5 mM $MgCl_2$, 10 mM KCl, 0.5 mM DTT, 330 mM sucrose, and protease inhibitors) and layered over sucrose buffer (880 mM sucrose, 0.5 mM $MgCl_2$, and protease inhibitors). The nuclear fraction was centrifuged at 13,200 rpm for 30 min. Nuclei were then lysed with nucleoplasmic extraction buffer (20 mM HEPES [pH 7.9], 1.5 mM $MgCl_2$, 150 mM KCl, 0.5 mM DTT, 0.2 mM EDTA, 10% glycerol, and protease inhibitors), sonicated, and centrifuged. After centrifuging at 15,000 × g for 20 min, the supernatant was recovered.

Immunoblotting

Cells were lysed in RIPA lysis buffer (50 mM Tris-HCl [pH 7.5], 150 mM NaCl, 1% NP-40, 0.1% SDS, and 1% sodium deoxycholate) supplemented with protease inhibitors (Roche), sonicated, and centrifuged at 13,200 rpm for 15 min. Protein concentrations were measured using the Dc-Protein Kit (Bio-Rad). Equal amounts of protein were separated on SDS-PAGE, blotted, probed for target proteins, and detected using ECL (Perkin Elmer). The primary antibodies used for detection were UBF (F-9; Santa Cruz Biotechnology), RRN3 (ab112052; Abcam), TAF1C (ab134394; Abcam), POLR1A/RPA194 (C-1; Santa Cruz Biotechnology), POLR1B/RPA135 (H-15; Santa Cruz Biotechnology), RPA43 (HPA022416; Sigma-Aldrich), α-tubulin (10D8; Santa Cruz Biotechnology), lamin A/C (H-110; Santa Cruz Biotechnology), and GAPDH (14C10; Cell Signaling Technology). Horseradish peroxidase (HRP)-conjugated secondary antibodies were from DAKO or Santa Cruz Biotechnology. Protein densitometry analysis was conducted using ImageJ software, and the mean value normalized with loading control was used as final protein band quantification.

qPCR and ChIP

qPCR for the mammalian cells was conducted essentially as described in Peltonen et al. (2014a). The following primers were used: POLR1B (forward GCCCAGCGGGCCTAGCCTAA, reverse TGATATCAGCCTGCACCGCGA), 5′ETS (forward +21 CGACCTGTCGTCGGAGAG, reverse +82 GGTCACCGT GAGGCCAGA; forward +1902 ATGGACGAGAATCACGAGCG, reverse +1952 CAGCCACGAACCCGACAC; forward +3288 GAAGCGTCGCGGGTCT, reverse +3433 CACGCGACACGACCAC). Isolation of chromatin, immunoprecipitation, and qPCR to detect rDNA sequences was as described in Peltonen et al. (2014a).

Yeast Strains and Spot Assay

The following yeast strains were used: DAS217: *MAT α ade2-1 ura3-1 trp1-1 leu2-3,112 his3-11,15 can1-100*; DAS1064: same as DAS217, but *rpa190-F1205H*; DAS178: same as DAS217, but *MAT a* and *rpa135-D784G*; DAS659: same as DAS217, but *MAT a* and *rrn3-S213P*; DAS937: same as DAS217, but *A190-3HA7his::LEU2*; DAS1061: same as DAS1064, but *A190-3HA7his::URA3*; DAS1062: same as DAS178, but *A190-3HA7his::URA3*; and DAS1063: same as DAS659, but *A190-3HA7his::URA3*. For the spot assay,

the cultures were grown in YEPD liquid media and harvested. For the spot assay, 10-fold dilutions were made, the first being 0.1 A_{600}, and 5 μL per dilution was plated on YEPD plates containing indicated concentrations of BMH-21. Plates were incubated at 30°C for 3 days.

Preparation of Yeast Lysates and Western Analysis

Cells were grown in YEPD and, in early log phase, were treated with 50 μM BMH-21 in 0.1 M NaH_2PO_4 or an equivalent volume of the vehicle. Ten milliliters of culture was harvested via centrifugation and washed with cold RIPA buffer. Cells were lysed using a FastPrep homogenizer. Samples were loaded onto 8% polyacramide gels, transferred to polyvinylidene difluoride (PVDF) membranes, and probed with antibodies (α-HA 12CA5 from Sigma-Aldrich to visualize A190 and α-Pgk1 22C5D8 from Thermo Fisher Scientific to visualize PGK1). A secondary α-mouse IgG conjugated to HRP (A9044; Sigma-Aldrich) was used for detection. Western blots were visualized with chemiluminescence (Chemidoc; Bio-Rad), and analyzed using Image Lab software.

Yeast RNA Isolation and RT-qPCR

Cells were grown in YEPD and, in early log phase, were treated with 50 μM BMH-21 in 0.1 M NaH_2PO_4 or an equivalent volume of the vehicle. One milliliter of culture was flash-frozen in a dry ice/ethanol bath. Cells were lysed using hot phenol lysis, and RNA was purified with acidic phenol/chloroform extraction followed by precipitation in 1 M ammonium acetate in ethanol. cDNA was synthesized using the SuperScript First-Strand Synthesis system (Thermo Fisher Scientific). qPCR was performed using probes for ITS1, 5′ETS, ACT1, and 18S rRNA using the ViiA 7 Real Time PCR system (Thermo Fisher Scientific), and data were analyzed using QuantStudio Real-Time PCR Software. The following primers were used: ITS1 forward 5′-TGGGCAAGAAGA CAAGAGATGGAG-3′; reverse 5′-GTTTGTGTTTGTTACCTCTGGGCC-3′; 5′-ETS forward 5′-AATAGCCGGTCGCAAGACT-3′; reverse 5′-TCACGGAATGG TACGTTTGA-3′; *ACT1* forward 5′-TCCGGTGATGGTGTTACTCA-3′; reverse 5′-GGCCAAATCGATTCTCAAAA-3′; 18S forward 5′-TGGCCTACCATGGTTT CAA-3′; reverse 5′-CTTGGATGTGGTAGCCGTTT-3′.

In Vitro Transcription

Assays for transcription elongation by Pol I were performed as described previously (Viktorovskaya et al., 2013) with the notable exception that BMH-21 was added to a final concentration of 1 μM to the synchronized elongation complexes (after initiation of transcription but prior to CTP release). An equal volume of vehicle (DMSO) was added to control samples.

Statistical Methods

The following statistical methods were used: Student's two-tailed t test, Dunnett's multiple-comparison test, and one-way ANOVA; p values less than 0.05 were considered significant. The method used is indicated in each figure legend.

SUPPLEMENTAL INFORMATION

ACKNOWLEDGMENTS

AUTHOR CONTRIBUTIONS

Methodology and Experimentation, T.W., S.M.N, H.L., K.P., A.K., and D.A.S.; Writing, T.W., S.M.N., D.A.S., and M.L.; Funding Acquisition and Supervision, D.A.S. and M.L.

DECLARATION OF INTERESTS

M.L. and K.P. hold patents on BMH-21, which are managed by The Johns Hopkins University. The other authors declare no competing interests.

REFERENCES

Andrews, W.J., Panova, T., Normand, C., Gadal, O., Tikhonova, I.G., and Panov, K.I. (2013). Old drug, new target: ellipticines selectively inhibit RNA polymerase I transcription. J. Biol. Chem. *288*, 4567–4582.

Brown, R.V., Danford, F.L., Gokhale, V., Hurley, L.H., and Brooks, T.A. (2011). Demonstration that drug-targeted down-regulation of MYC in non-Hodgkins lymphoma is directly mediated through the promoter G-quadruplex. J. Biol. Chem. *286*, 41018–41027.

Burger, K., Mühl, B., Harasim, T., Rohrmoser, M., Malamoussi, A., Orban, M., Kellner, M., Gruber-Eber, A., Kremmer, E., Hölzel, M., and Eick, D. (2010). Chemotherapeutic drugs inhibit ribosome biogenesis at various levels. J. Biol. Chem. *285*, 12416–12425.

Bywater, M.J., Poortinga, G., Sanij, E., Hein, N., Peck, A., Cullinane, C., Wall, M., Cluse, L., Drygin, D., Anderes, K., et al. (2012). Inhibition of RNA polymerase I as a therapeutic strategy to promote cancer-specific activation of p53. Cancer Cell *22*, 51–65.

Bywater, M.J., Pearson, R.B., McArthur, G.A., and Hannan, R.D. (2013). Dysregulation of the basal RNA polymerase transcription apparatus in cancer. Nat. Rev. Cancer *13*, 299–314.

Claypool, J.A., French, S.L., Johzuka, K., Eliason, K., Vu, L., Dodd, J.A., Beyer, A.L., and Nomura, M. (2004). Tor pathway regulates Rrn3p-dependent recruitment of yeast RNA polymerase I to the promoter but does not participate in alteration of the number of active genes. Mol. Biol. Cell *15*, 946–956.

Colis, L., Peltonen, K., Sirajuddin, P., Liu, H., Sanders, S., Ernst, G., Barrow, J.C., and Laiho, M. (2014a). DNA intercalator BMH-21 inhibits RNA polymerase I independent of DNA damage response. Oncotarget *5*, 4361–4369.

Colis, L., Ernst, G., Sanders, S., Liu, H., Sirajuddin, P., Peltonen, K., DePasquale, M., Barrow, J.C., and Laiho, M. (2014b). Design, synthesis, and structure-activity relationships of pyridoquinazolinecarboxamides as RNA polymerase I inhibitors. J. Med. Chem. *57*, 4950–4961.

Drygin, D., Rice, W.G., and Grummt, I. (2010). The RNA polymerase I transcription machinery: an emerging target for the treatment of cancer. Annu. Rev. Pharmacol. Toxicol. *50*, 131–156.

Drygin, D., Lin, A., Bliesath, J., Ho, C.B., O'Brien, S.E., Proffitt, C., Omori, M., Haddach, M., Schwaebe, M.K., Siddiqui-Jain, A., et al. (2011). Targeting RNA polymerase I with an oral small molecule CX-5461 inhibits ribosomal RNA synthesis and solid tumor growth. Cancer Res. *71*, 1418–1430.

Engel, C., Sainsbury, S., Cheung, A.C., Kostrewa, D., and Cramer, P. (2013). RNA polymerase I structure and transcription regulation. Nature *502*, 650–655.

Fernández-Tornero, C., Moreno-Morcillo, M., Rashid, U.J., Taylor, N.M., Ruiz, F.M., Gruene, T., Legrand, P., Steuerwald, U., and Müller, C.W. (2013). Crystal structure of the 14-subunit RNA polymerase I. Nature *502*, 644–649.

Grummt, I. (2010). Wisely chosen paths—regulation of rRNA synthesis: delivered on 30 June 2010 at the 35th FEBS Congress in Gothenburg, Sweden. FEBS J. *277*, 4626–4639.

Guner, G., Sirajuddin, P., Zheng, Q., Bai, B., Brodie, A., Liu, H., Af Hällström, T., Kulac, I., Laiho, M., and De Marzo, A.M. (2017). Novel assay to detect RNA polymerase I activity *in vivo*. Mol. Cancer Res. *15*, 577–584.

Haag, J.R., and Pikaard, C.S. (2007). RNA polymerase I: a multifunctional molecular machine. Cell *131*, 1224–1225.

Martinez-Rucobo, F.W., and Cramer, P. (2013). Structural basis of transcription elongation. Biochim. Biophys. Acta *1829*, 9–19.

McStay, B., and Grummt, I. (2008). The epigenetics of rRNA genes: from molecular to chromosome biology. Annu. Rev. Cell Dev. Biol. *24*, 131–157.

Montanaro, L., Treré, D., and Derenzini, M. (2008). Nucleolus, ribosomes, and cancer. Am. J. Pathol. *173*, 301–310.

Morgado-Palacin, L., Llanos, S., Urbano-Cuadrado, M., Blanco-Aparicio, C., Megias, D., Pastor, J., and Serrano, M. (2014). Non-genotoxic activation of p53 through the RPL11-dependent ribosomal stress pathway. Carcinogenesis *35*, 2822–2830.

Mullineux, S.T., and Lafontaine, D.L. (2012). Mapping the cleavage sites on mammalian pre-rRNAs: where do we stand? Biochimie *94*, 1521–1532.

Peltonen, K., Colis, L., Liu, H., Jäämaa, S., Moore, H.M., Enbäck, J., Laakkonen, P., Vaahtokari, A., Jones, R.J., af Hällström, T.M., and Laiho, M. (2010). Identification of novel p53 pathway activating small-molecule compounds reveals unexpected similarities with known therapeutic agents. PLoS ONE *5*, e12996.

Peltonen, K., Colis, L., Liu, H., Trivedi, R., Moubarek, M.S., Moore, H.M., Bai, B., Rudek, M.A., Bieberich, C.J., and Laiho, M. (2014a). A targeting modality for destruction of RNA polymerase I that possesses anticancer activity. Cancer Cell *25*, 77–90.

Peltonen, K., Colis, L., Liu, H., Jäämaa, S., Zhang, Z., Af Hällström, T., Moore, H.M., Sirajuddin, P., and Laiho, M. (2014b). Small molecule BMH-compounds that inhibit RNA polymerase I and cause nucleolar stress. Mol. Cancer Ther. *13*, 2537–2546.

Popov, A., Smirnov, E., Kováčik, L., Raška, O., Hagen, G., Stixová, L., and Raška, I. (2013). Duration of the first steps of the human rRNA processing. Nucleus *4*, 134–141.

Richardson, L.A., Reed, B.J., Charette, J.M., Freed, E.F., Fredrickson, E.K., Locke, M.N., Baserga, S.J., and Gardner, R.G. (2012). A conserved deubiquitinating enzyme controls cell growth by regulating RNA polymerase I stability. Cell Rep. *2*, 372–385.

Russell, J., and Zomerdijk, J.C. (2006). The RNA polymerase I transcription machinery. Biochem. Soc. Symp. *73*, 203–216.

Schneider, D.A. (2012). RNA polymerase I activity is regulated at multiple steps in the transcription cycle: recent insights into factors that influence transcription elongation. Gene *493*, 176–184.

Schneider, D.A., and Nomura, M. (2004). RNA polymerase I remains intact without subunit exchange through multiple rounds of transcription in Saccharomyces cerevisiae. Proc. Natl. Acad. Sci. U S A *101*, 15112–15117.

Schneider, D.A., Michel, A., Sikes, M.L., Vu, L., Dodd, J.A., Salgia, S., Osheim, Y.N., Beyer, A.L., and Nomura, M. (2007). Transcription elongation by RNA polymerase I is linked to efficient rRNA processing and ribosome assembly. Mol. Cell *26*, 217–229.

Viktorovskaya, O.V., Engel, K.L., French, S.L., Cui, P., Vandeventer, P.J., Pavlovic, E.M., Beyer, A.L., Kaplan, C.D., and Schneider, D.A. (2013). Divergent contributions of conserved active site residues to transcription by eukaryotic RNA polymerases I and II. Cell Rep. *4*, 974–984.

Warner, J.R., Vilardell, J., and Sohn, J.H. (2001). Economics of ribosome biosynthesis. Cold Spring Harb. Symp. Quant. Biol. *66*, 567–574.

Wilson, M.D., Harreman, M., and Svejstrup, J.Q. (2013). Ubiquitylation and degradation of elongating RNA polymerase II: the last resort. Biochim. Biophys. Acta *1829*, 151–157.

Xu, H., Di Antonio, M., McKinney, S., Mathew, V., Ho, B., O'Neil, N.J., Santos, N.D., Silvester, J., Wei, V., Garcia, J., et al. (2017). CX-5461 is a DNA G-quadruplex stabilizer with selective lethality in BRCA1/2 deficient tumours. Nat. Commun. *8*, 14432.